# Research on Anti-icing Power of the Cable-Stayed Cylindrical Structure Based on PTC

Maozheng Wang[1], Xingliang Jiang[1], Yi Liao[1], Qin Hu[1], Hualong Zheng[1]

[1] *State Key Laboratory of Power Transmission Equipment & System Security and New Technology, Chongqing University, Chongqing,400044, China*

wangmaozheng@cqu.edu.cn, xljiang@cqu.edu.cn, liaoyi@cqu.edu.cn, huqin@cqu.edu.cn, hualong.zheng@cqu.edu.cn

*Abstract*— **In winter, freezing rain often falls in southern China, and the cable-stayed cylindrical structure will form ice edges on its surface under the influence of freezing rain; when freezing rain flows down the cable-stayed cylindrical structure, it will gradually freeze to form glaze, glaze grows through wet to form ice ridges. Under the action of gravity and wind, the ice edge will fall downwards. When pedestrians and vehicles passing under the cable-stayed cylindrical structure, the falling ice edge will hurt the passing pedestrians and vehicles, causing traffic accidents. It seriously affects the normal driving of vehicles and endangers the safety of pedestrians. At present, the anti-icing measures for the cable-stayed cylindrical structure are not adequately done. Mostly, when the cable-stayed cylindrical structure produce ice edges, the ice edge is scraped off through the slip ring, and the anti-icing efficiency of this method is not high: on the one hand, it is necessary to wait for no pedestrians or vehicles under the cable-stayed cylindrical structure to scrape the ice edge; on the other hand, the scraping of the ice edge is not thorough enough and soon new ice ridges will be formed again. In this paper, polyester film is used as the substrate, graphene is used as the conductive filler, n-tetradecane is added to reduce the Curie temperature point, and a new type of organic PTC film is made. The new organic PTC material film is coated on the surface of the cable-stayed cylindrical structure. By changing the diameter of the cylindrical structure, the anti-icing power of the cable-stayed cylindrical structure with different diameters is studied. Through the research, it is found that with the increase of the diameter of the cable-stayed cylindrical structure, the anti-icing power of the cable-stayed cylindrical structure per unit area will gradually decrease, and finally tend to be stable, On the one hand, with the increase of the diameter of the cable-stayed cylindrical structure, it will be more difficult for freezing rain to form glaze, so that the lower anti-icing power can prevent the formation of ice edges; on the other hand, with the increase of the diameter of the cylinder, the air flow field around it will be distorted to a certain extent. After the diameter of the cable-stayed cylindrical structure increases to a certain extent, the difficulty of forming the glaze and the distortion of the air flow field will not increase, and the anti-icing power will remain basically unchanged; The ambient temperature is constant, the higher the wind speed, the higher the anti-icing power of the cable-stayed cylindrical structure per unit area. In this paper, the research on the anti-icing power of the PTC cable-stayed cylindrical structure provides power parameters for the subsequent design of the anti-icing device based on the PTC cable-stayed cylindrical structure.**

Keywords—***Cable-stayed; Cylindrical structure; Graphene; PTC; Anti-icing power***

## I. Introduction

Ice cover on structure is a comprehensive physical phenomenon influenced by temperature, humidity, cold and warm air convection, circulation and wind[1]. Every year in the cold winter or just after spring, the warm and humid airflow from the north and the south meets the cold air, and an inversion phenomenon occurs, where the top to the bottom of the atmosphere is below zero, above zero, and below zero regions, and the part above zero is called the inversion layer. Warm and humid airflow from the ground began to cool after rising to the region. Water vapor in the process of continuous condensation formed ice crystals. Snowflakes or overcooled water droplets, into the inversion layer, basically all transformed into overcooled water droplets, and that overcooled water droplets landing will form freezing rain. In winter, Chinese southern regions will be freezing rain from time to time, and the cable-stayed cylindrical structure affected by freezing rain on its surface will form ice prisms: when freezing rain flows downward along the cylindrical structure, it will gradually freeze to form glaze, and glaze will form the ice edge through wet growth. The ice edge fall under external factors such as rising temperature, wind blowing or normal vibration of cylindrical structure. When pedestrians and vehicles passing under the cable-stayed cylindrical structure, the falling ice edge will hurt the passing pedestrians and vehicles, causing traffic accidents. It seriously affects the normal driving of vehicles and endangers the safety of pedestrians.

Scholars at home and abroad have conducted a lot of research on ice-covering of the cable-stayed cylindrical structure. Li Shouying et al[2]conducted wind tunnel experimental to study on the vibration characteristics of crescent-shaped, fan-shaped and D-shaped ice-covered cable-stayed respectively. The results showed that under ice-covered conditions the critical wind velocity of the cable's galloping oscillation is lower, and the probability of galloping oscillation is higher. Tan Dongmei et al[3]used Fluent fluid analysis software to study the aerodynamic characteristics of a three-dimensional fan-shaped ice-covered cable-stayed, and derived the galloping oscillation force coefficients based on the derived three-part force coefficients. The results show that the fan-shaped ice overlay does not cause the stayed cable to undergo galloping oscillation. Teng Erfu et al[4]used Fluent fluid analysis software to simulate the

aerodynamic parameters of crescent-shaped ice-covered conductors and compared them with the wind tunnel test results, and the results were in good agreement. Wang Kaili et al[5]did a numerical wind tunnel study on two types of ice-covered sections of stayed cable. The results showed that wind speed, ice cover type and wind angle of attack all have a large effect on the three-part force coefficient of the cable-stayed, and there is a possibility of galloping oscillation. Kollár et al[6]studied the effect of parameters such as raindrop particle size, wind angle, tilt angle, and temperature on the quality and shape of cylindrical ice cover. Demartino et al[7]et al. conducted a wind tunnel experimental study of two ice-cover models and predicted the galloping oscillation instability based on a quasi-steady-state approach. Huang Tao[8]did wind tunnel tests on six types of cable-stayed over ice models to obtain the variation law of their aerodynamic coefficients. The results showed that the average lift coefficients of all six models would drop abruptly, leading to an increase in the interval of their galloping oscillation force coefficients less than zero and an increase in the probability of galloping oscillation.

At present, scholars at home and abroad are focused on the research of ice-covering of the cable-stayed cylindrical structure and their characteristics after ice-covering, and there is no research on ice-proofing of the cable-stayed cylindrical structure. In this paper, polyester film is used as the substrate, graphene is used as the conductive filler, n-tetradecane is added to reduce the Curie temperature point, and a new type of organic PTC film is made. The new organic PTC material film is coated on the surface of the cable-stayed cylindrical structure. By changing the diameter of the cylindrical structure, the anti-icing power of the cable-stayed cylindrical structure with different diameters is studied. The anti-icing power of the cable-stayed cylindrical structure is investigated through field tests and numerical simulations, and the critical anti-icing power of the cable-stayed cylindrical structure with different diameters is obtained, which provides power parameters for the subsequent design of anti-icing devices based on the PTC cable-stayed cylindrical structure.

## II. NATURE TEST

In this paper, polyester film is used as the substrate, graphene is used as the conductive filler, n-tetradecane is added to reduce the Curie temperature point, and a new type of organic PTC film is made. The new organic PTC film is coated on the surface of the cable-stayed cylindrical structure, and the temperature sensor is attached to the organic PTC film on the windward side to monitor the surface temperature of the organic PTC film in real time. The critical anti-icing power of the cable-stayed cylindrical structure is studied through field tests at the Xue Feng Mountain Energy Equipment Safety Field Scientific Observation and Research Station.

### A. Critical Anti-icing Power of the Cable-Stayed Cylindrical Structure with Different Diameters

The cable-stayed cylindrical structure were placed at an angle of 30° to the horizontal and perpendicular to the wind direction. The critical anti-icing power of the cable-stayed cylindrical structure with different diameters was

experimentally studied by changing the diameters of the cable-stayed cylindrical structure, as shown in Fig. 1.



a)    75mm

b)    90mm

c)    110mm

d)    125mm

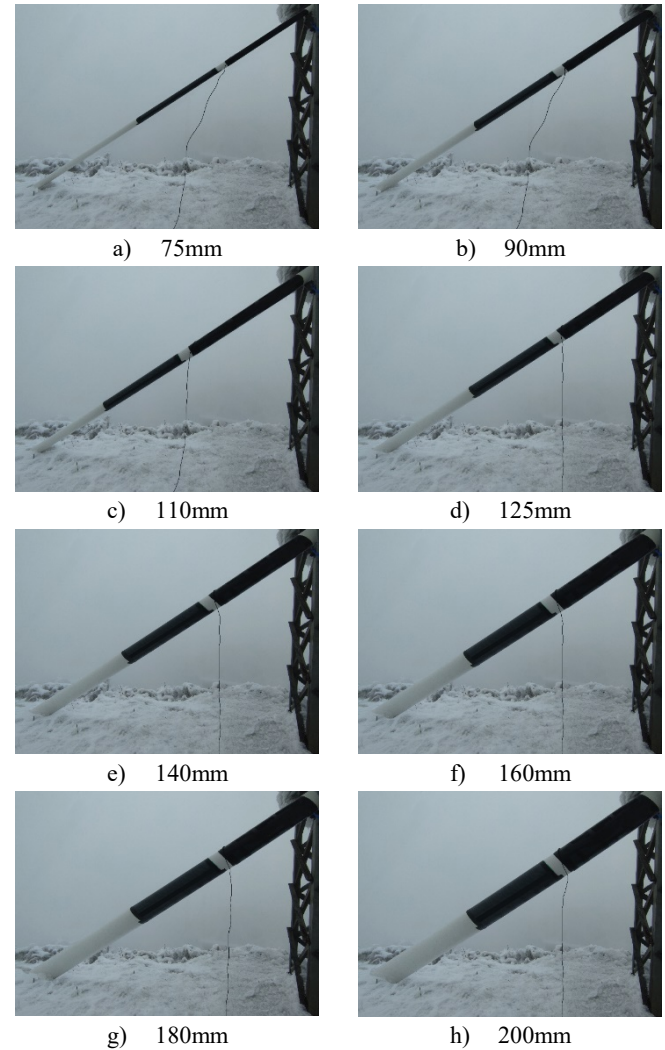e)    140mm

f)    160mm

g)    180mm

h)    200mm

Fig. 1 Different diameters of the cable-stayed cylindrical structure

The organic PTC electric heating film is powered by the regulator. Adjust the regulator, the working voltage of the organic PTC electric heating film changing, and the power of the organic PTC electric heating film changing. When the surface temperature of the windward side of the organic PTC electric heating film is about 1℃, this state is considered to be the critical state, and the regulator output power in this state is the critical anti-icing power of the cable-stayed cylinder structure. Through continuous tests, the critical anti-icing power of the cable-stayed cylindrical structure of different diameters was obtained at an ambient temperature of -3.3℃, a wind speed of 11.2 m/s, a relative humidity of 0.99, and an atmospheric pressure of 86 kPa. The fitted curves of the variation of the critical anti-icing power with the diameter of the cable-stayed cylindrical structure under this ambient condition were plotted, as in Fig. 2.

It can be seen from Fig. 2 that the critical anti-icing power gradually decreases with the increase of the diameter of the cable-stayed cylindrical structure, and the trend of decreasing critical anti-icing power gradually flattens out when the diameter of the cable-stayed cylindrical structure increases to a certain degree. The reason for this analysis may be because the larger the diameter of the cable-stayed cylindrical

structure, the smaller the probability of water droplets colliding with the cable-stayed cylindrical structure [9].
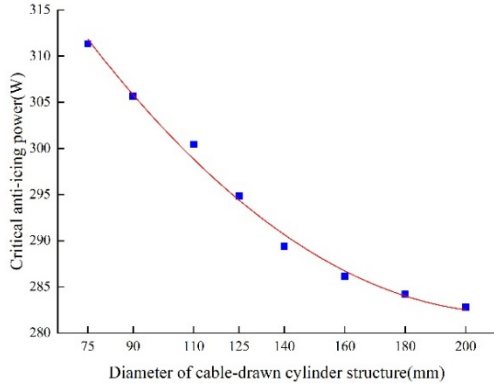


Fig. 2 The variation of the critical anti-icing power with the diameter of the cable-stayed cylindrical structure

## B. Critical Anti-icing Power of the Cable-Stayed Cylindrical Structure with Different Placement Angles

Taking the 110mm cable-stayed cylindrical structure as an example, the cable-stayed cylindrical structure was placed perpendicular to the wind direction and its horizontal angle was changed to study the critical anti-icing power of the cable-stayed cylindrical structure under different placement angles. At an ambient temperature of -3.3°C, a wind speed of 11.2m/s, a relative humidity of 0.99, and an atmospheric pressure of 86kPa, the 110mm cable-stayed cylindrical structure was placed at 30°, 45°, and 60°, as shown in Fig. 3.
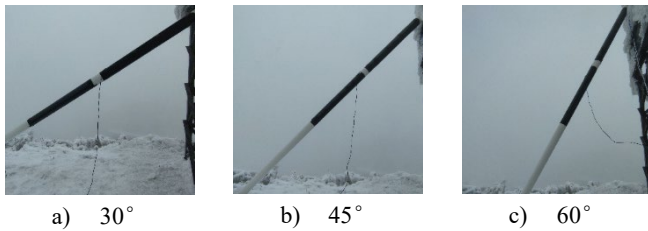


a)  30°      b)  45°      c)  60°

Fig. 3 Different angles of the cable-stayed cylindrical structure

By adjusting the regulator, the critical anti-icing power of the cable-stayed cylindrical structure under different placement angles is obtained, and the fitted curve of the critical anti-icing power with the change of placement angle is drawn, as in Fig. 4.
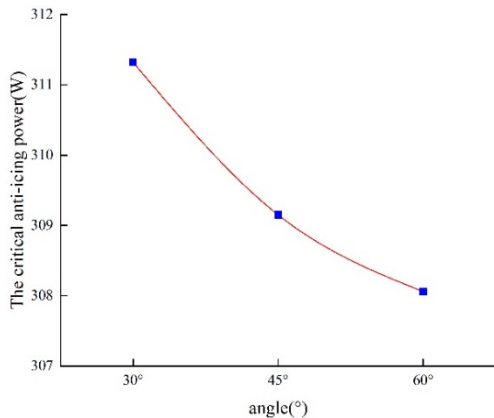


Fig. 4 The variation of the critical anti-icing power with the angle of the cable-stayed cylindrical structure

It can be seen from Fig. 4 that the critical anti-icing power of the cable-stayed cylindrical structure gradually decreases as the placement angle increases.

## C. Critical Anti-icing Power of the Cable-Stayed Cylindrical Structure under Different Wind Speeds

Taking the 110mm cable-stayed cylindrical structure as an example, the cable-stayed cylindrical structure was placed at an angle of 30° with the horizontal and perpendicular to the wind direction. At an ambient temperature of -3.3°C, a relative humidity of 0.99, and an atmospheric pressure of 86 kPa the critical anti-icing power of the cable-stayed cylindrical structure under different wind speeds was obtained experimentally by adjusting the regulator, and plotting the critical anti-icing power with wind speed fitting curve, as in Fig. 5.
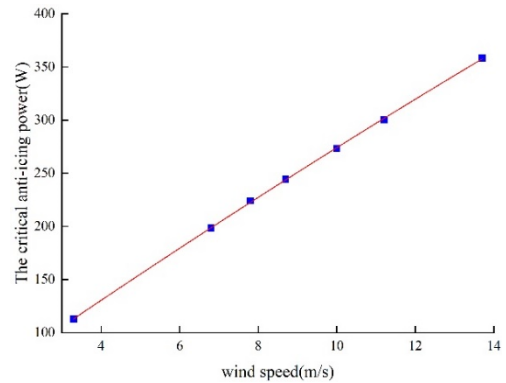


Fig. 5 The variation of the critical anti-icing power with the wind speed

It can be seen from Fig. 5 that the critical anti-icing power of the cable-stayed cylindrical structure increases basically linearly with the increase of wind speed.

## III. NUMERICAL SIMULATION

### A. Anti-icing Model for the Cable-Stayed Cylindrical Structure

1) *Model Assumptions:* Considering the flow and temperature field characteristics of the cable-stayed cylindrical structure in the organic PTC electric heating film anti-icing environment, the following assumptions are made in the numerical simulation study of the cable-stayed cylindrical structure for anti-icing in this paper:

- Disregarding the phase change phenomenon of water droplets freezing on the surface of the organic PTC heating film.
- Considering the effect of water droplet properties on anti-icing by converting the water droplet properties in cold fluids to the thermal physical parameters of wet air.
- Assuming that the fluids are incompressible.

2) *Critical anti-icing power:* In the critical anti-icing state, the heat balance equation of the surface of the cable-stayed cylindrical structure can be expressed as:

$$P_d + P_v + P_k = P_c + P_r \qquad (2\text{-}1)$$

Where: $P_d$ is the heating power of PTC electric film, namely the critical anti-icing power; $P_v$ is the frictional heating power of the air flow on the surface of the cable-stayed cylindrical structure. In the critical anti-icing state, the power order of magnitude is small and can be ignored; $P_k$ is the kinetic energy of the impact when the liquid droplet hits the surface of the cable-stayed cylindrical structure; $P_c$ is the convective heat transfer power between the surface of the

cable-stayed cylindrical structure and the air; $P_r$ is the radiation heat dissipation power of the surface of the cable-stayed cylindrical structure. In the critical anti-icing state, the power order of magnitude is small and can be ignored.

The impact kinetic energy $P_k$ of water droplets when they collide with the surface of the cable-stayed cylindrical structure can be obtained from the following equation:

$$P_k = \frac{1}{2} S_p \alpha_1 \alpha_2 w u^3 \tag{2-2}$$

Where, $S_p$ is the projected area of the cable-stayed cylindrical structure in the direction of incoming flow; $\alpha_1$ is the droplet collision coefficient. The relationship between droplet collision coefficient and wind speed and median volume diameter($MVD$) of droplet is shown in Fig. 6; $\alpha_2$ is the capture rate of water droplets. In the critical anti-icing state, there is a water film on the surface of the cable-stayed cylindrical structure, so the capture rate of water droplets on the surface of the cable-stayed cylindrical structure is 1; $w$ is the liquid water content in the air; $u$ is the wind speed.
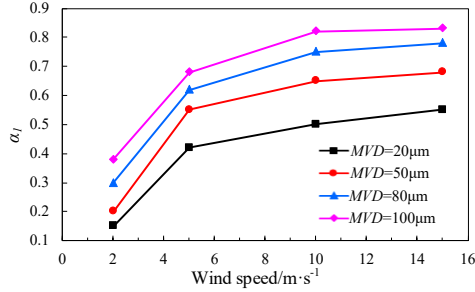


Fig. 6 The relationship between $\alpha_1$ and $u$ and $MVD$

Convective heat transfer power $P_c$ consists of forced convection heat transfer and natural convection heat transfer. According to the heat transfer theory, the cable-stayed cylindrical structure can be regarded as a circular tube model, and its convective heat transfer power can be expressed as:

$$P_c = hA\Delta t_m \tag{2-3}$$

Where, $h$ is the convective heat transfer coefficient; $A$ is the heat transfer area; $\Delta t_m$ is the temperature difference on the heat transfer area, which is always positive.

$$h = k_w \left( N_{Un} + N_{Uf} \right) / L \tag{2-4}$$

$$N_{Un} = B(GrPr)^b \tag{2-5}$$

$$N_{Uf} = CR_c^n P_r^{1/3} \tag{2-6}$$

Where, $k_w$ is the thermal conductivity of wet air; $N_{Un}$ is the Nusselt number representing natural convection intensity; $N_{Uf}$ is the Nusselt number representing forced convection intensity; $L$ is model characteristic length; $Gr$ is the Lagshev number; $Pr$ is the Prandtl number; $Re$ is the Reynolds number; $B$ and $b$ are coefficients determined by $Gr$ and $Pr$, as shown in Table I; $C$ and $n$ are the coefficients determined by $Re$, as shown in TableII.

TABLE I The Relationship Between $B$, $b$ AND $Gr$

| $Gr$ | $B$ | $b$ |
|---|---|---|
| $1.43\times10^4 \leqslant Gr < 3\times10^9$ | 0.59 | 0.25 |
| $3\times10^9 \leqslant Gr \leqslant 2\times10^{10}$ | 0.0292 | 0.39 |
| $Gr > 2\times10^{10}$ | 0.11 | 1/3 |

TABLE II The Relationship Between $C$, $n$ AND $Re$

| $Re$ | $C$ | $n$ |
|---|---|---|
| $4 \leqslant Re \leqslant 40$ | 0.911 | 0.385 |
| $40 \leqslant Re \leqslant 4000$ | 0.683 | 0.466 |
| $4000 \leqslant Re \leqslant 40000$ | 0.193 | 0.618 |
| $40000 \leqslant Re \leqslant 400000$ | 0.0262 | 0.805 |

$$Gr = \frac{g\Delta t_m L^3}{v^2 \left[ (T_i + T_\infty)/2 + 273.15 \right]} \tag{2-7}$$

$$Pr = \frac{\mu C_p}{k} \tag{2-8}$$

$$N_{Uf} = CR_c^n P_r^{1/3} \tag{2-9}$$

Where, $g$ is the acceleration of gravity; $v$ is the kinematic viscosity of air; $T_i$ is the temperature of the surface of the cable-stayed cylindrical structure; $T_\infty$ is the ambient temperature; $\mu$ is the dynamic viscosity coefficient of air; $C_p$ is the specific heat capacity of air at constant pressure; $\rho_w$ is the density of wet air; $u$ is the wind speed.

*3) Wet Air Parameters:* The density of wet air is calculated as Eq. 2-10:

$$\rho_w = \frac{p_w}{R_d T} \frac{0.001d + 1}{(0.001606d + 1)} \tag{2-10}$$

Where, $\rho_w$ is the density of wet air, kg/m³; $p_w$ is the total pressure of wet air, take 101325Pa; $R_d$ is the gas constant of dry air, take 287J/(kg·K); $T$ is the temperature of wet air, K; $d$ is the moisture content of wet air, g/kg, and the value can be calculated by Eq. 2-11:

$$d = \frac{622\varphi p_{sat}}{p_w - \varphi p_{sat}} \tag{2-11}$$

Where, $\varphi$ is the relative humidity of the wet air, %, which can be transformed by the subsequent calculation; $p_{sat}$ is the water vapor saturation pressure corresponding to the wet air temperature T, Pa, and the value can be calculated by fitting Eq. 2-12:

$$p_{sat} = e^{7.23\times10^{-7}(T-273.15)^3 - 2.71\times10^{-4}(T-273.15)^2 + 7.2\times10^{-2}(T-273.15) + 6.42} \tag{2-12}$$

The thermal conductivity of wet air is calculated as Eq. 2-13:

$$k_w = \frac{k_d}{dA_{d,v}M_d/M_v + 1} + \frac{dk_v}{A_{v,d}M_v/M_d + d} \tag{2-13}$$

Where, $k_w$ is the thermal conductivity of wet air, W/(m k); $M_d$ is the molecular weight of dry air, take 28.97; $M_v$ is the molecular weight of water vapor, take 18.02; $k_d$ is the thermal conductivity of dry air, W/(m k), and the value can be calculated by fitting Eq. 2-14; $k_v$ is the thermal conductivity of water vapor, W/(m k), and the value can be calculated by fitting Eq. 2-15; $A_{d,v}$ is the combination factor of dry air and water vapor, and the value can be calculated by Eq. 2-16; $A_{v,d}$ is the combination factor of water vapor and dry air, and the value can be calculated by Eq. 2-17.

$$k_d = \left( -3\times10^{-7}(T-273.15)^2 + 7.7\times10^{-3}(T-273.15) + 2.44 \right)\times10^{-2} \tag{2-14}$$

$$k_v = \left( 1\times10^{-5}(T-273.15)^2 + 5.2\times10^{-3}(T-273.15) + 1.83 \right)\times10^{-2} \tag{2-15}$$

$$A_{d,v} = \left( 0.8881\sqrt{\mu_d/\mu_v} + 1 \right)^2 \tag{2-16}$$

$$A_{v,d} = \frac{A_{d,v}\mu_v M_d}{\mu_d M_v} \qquad (2\text{-}17)$$

### B. Simulation of Critical Anti-icing of the Cable-Stayed Cylindrical Structure

In this paper, the critical state of the organic PTC electric heating film surface temperature of about 1°C is used to determine its critical anti-icing power. Combined with Eq. 2-1 - Eq. 2-17, a heat - moisture - flow coupling model is established, and the multiphysics field modeling and simulation software COMSOL Multiphysics is used for simulation analysis.

*1) Simulation of Critical Anti-icing of the Cable-Stayed Cylindrical Structure with Different Diameters:* Field tests were conducted at the Xue Feng Mountain Energy Equipment Safety Field Scientific Observation and Research Station to measure the critical anti-icing power of different diameters of the cable-stayed cylindrical structure when they were placed at an angle of 30° to the horizontal, with an ambient temperature of -3.3°C, wind speed of 11.2m/s, relative humidity of 0.99, and atmospheric pressure of 86kPa. With this critical anti-icing power as the excitation, the heat-humidity-flow coupled field simulation study is carried out to obtain the temperature field of organic PTC electric heating film on the outer side of the cable-stayed cylindrical structure with different diameters, as in Fig. 7 and the air flow field of the cross section in parallel wind speed direction of the cable-stayed cylindrical structure with different diameters, as in Fig. 8.
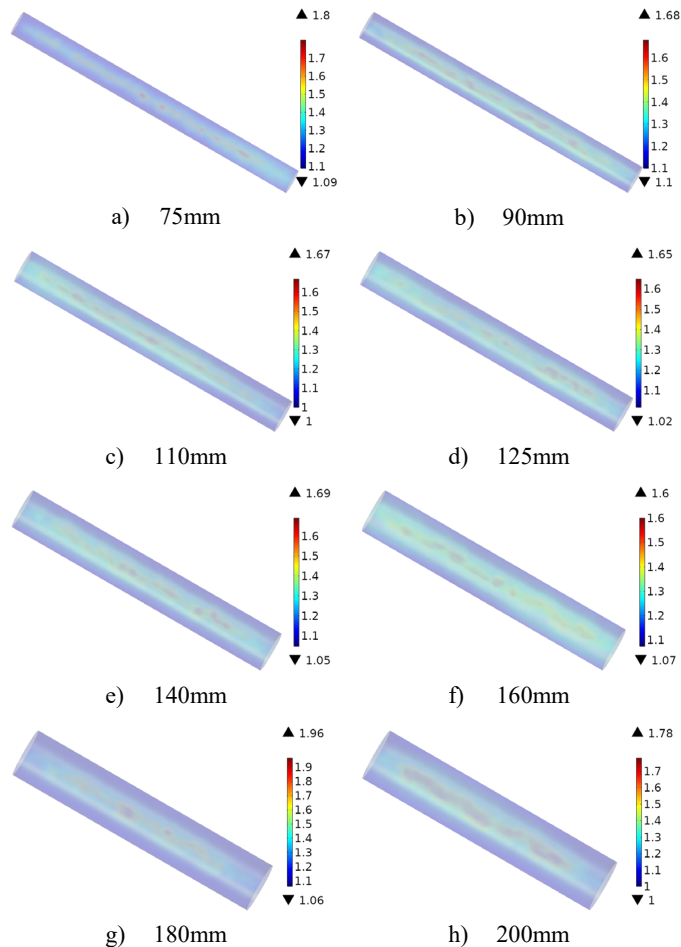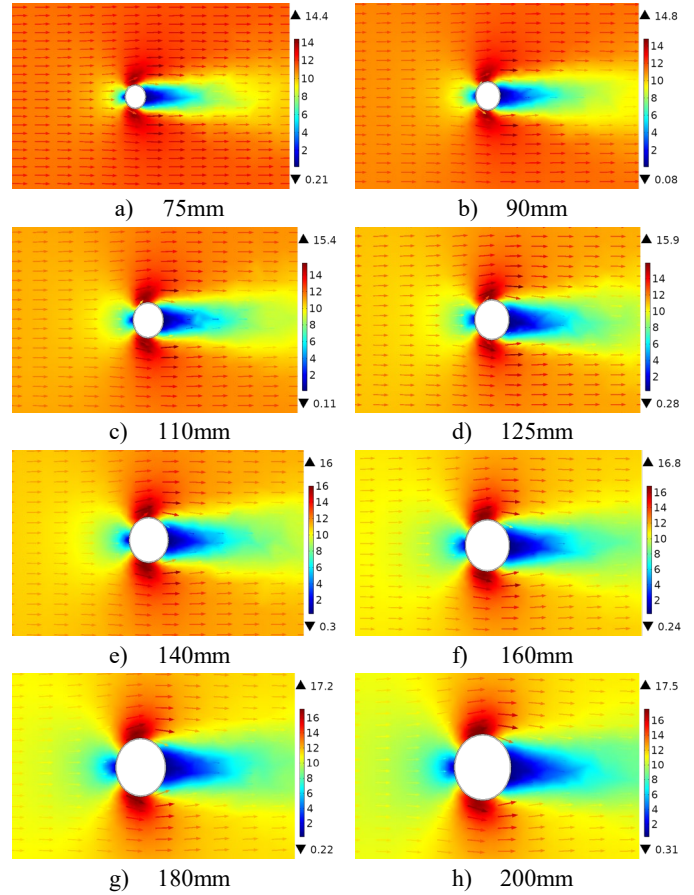
Fig. 7 The temperature field of organic PTC electric heating film on the outer side of the cable-stayed cylindrical structure with different diameters



a)    75mm



b)    90mm



c)    110mm



d)    125mm



e)    140mm



f)    160mm



g)    180mm



h)    200mm

Fig. 8 The air flow field

It can be seen from Fig. 8 that under the action of the same wind speed, the larger the diameter of the cable-stayed cylindrical structure is, the greater the local maximum wind speed is. The larger the diameter of the cable-stayed cylindrical structure is, the greater the range of the small wind speed on the windward side and the leeward side is, resulting in the probability of water droplets colliding with the cable-stayed cylindrical structure becoming smaller, so the moisture content of its surface is lower. The moisture evaporation heat absorption is lower, and the critical anti-icing power is reduced.

*2) Simulation of Critical Anti-icing of the Cable-Stayed Cylindrical Structure with Different Placement Angles:* Field tests were conducted at the Xue Feng Mountain Energy Equipment Safety Field Scientific Observation and Research Station. Taking the 110mm cable-stayed cylindrical structure as an example, placing it perpendicular to the wind direction and changing its horizontal angle, the critical anti-icing power of the cable-stayed cylindrical structure was measured at different angles of placement at an ambient temperature of -3.3℃, a wind speed of 11.2m/s, a relative humidity of 0.99, and an atmospheric pressure of 86kPa. With this critical anti-icing power as the excitation, the heat-humidity-flow coupled field simulation study is carried out to obtain the temperature field of organic PTC electric heating film on the outside of the cable-stayed cylindrical structure at different placement angles, as in Fig. 9, and the air flow field of the cross section

in the parallel wind speed direction at different placement angles, as in Fig. 10.
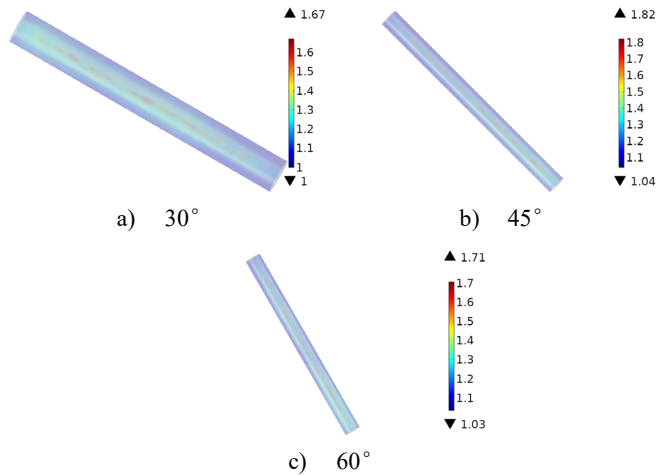


a) 30°                b) 45°

c) 60°

Fig. 9 The temperature field of organic PTC electric heating film on the outer side of the cable-stayed cylindrical structure at different placement angles



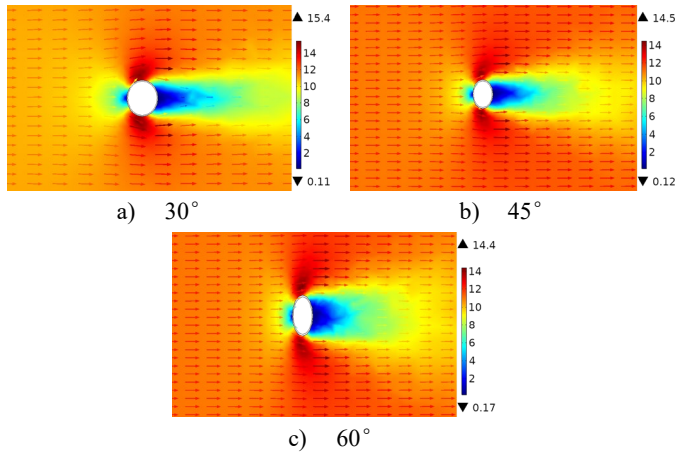a) 30°                b) 45°

c) 60°

Fig. 10 The air flow field

It can be seen from Fig. 10 that under the action of the same wind speed, the local maximum wind speed of the cable-stayed cylindrical structure with different placement angles is basically the same. The larger the placement angle of the cable-stayed cylindrical structure is, the greater the range of the small wind speed on the windward side and the leeward side is, resulting in the probability of water droplets colliding with the cable-stayed cylindrical structure becoming smaller, so the moisture content of its surface is lower. The moisture evaporation heat absorption is lower, and the critical anti-icing power is reduced.

*3) Simulation of Critical Anti-icing of the Cable-Stayed Cylindrical Structure under Different Wind Speeds:* Field tests were conducted at the Xue Feng Mountain Energy Equipment Safety Field Scientific Observation and Research Station. Taking the 110mm cable-stayed cylindrical structure as an example and placing it perpendicular to the wind direction, at a placement angle of 30°, an ambient temperature of -3.3°C, a relative humidity of 0.99, and an atmospheric pressure of 86 kPa, the critical anti-icing power of the cable-stayed cylindrical structure was measured at different wind speeds. With this critical anti-icing power as the excitation, the heat-humidity-flow coupled field simulation study is carried out to obtain the temperature field of organic PTC electric heating film on the outside of the

cable-stayed cylindrical structure at different wind speeds, as in Fig. 11, and the air flow field of the cross section in the parallel wind speed direction at different wind speeds, as in Fig. 12.
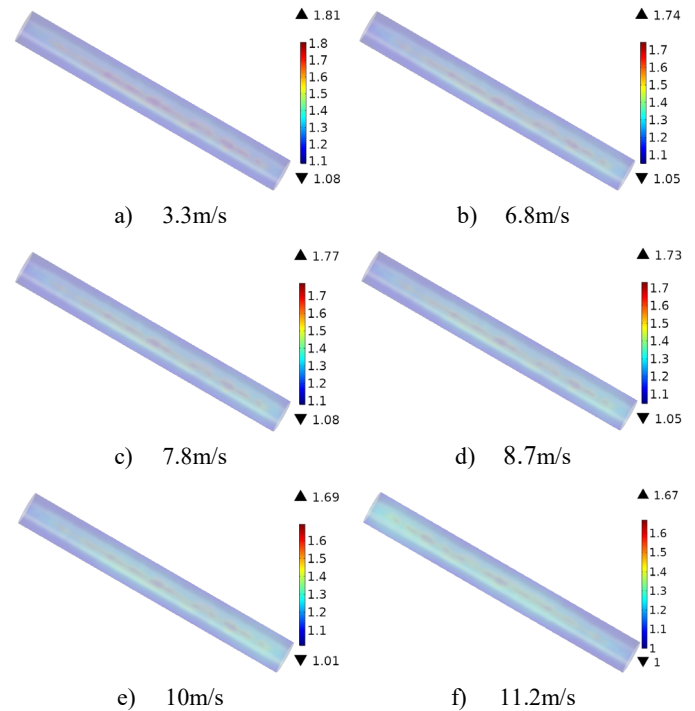


a) 3.3m/s              b) 6.8m/s

c) 7.8m/s              d) 8.7m/s

e) 10m/s               f) 11.2m/s

Fig. 11 The temperature field of organic PTC electric heating film on the outside of the cable-stayed cylindrical structure at different wind speeds



a) 3.3m/s              b) 6.8m/s

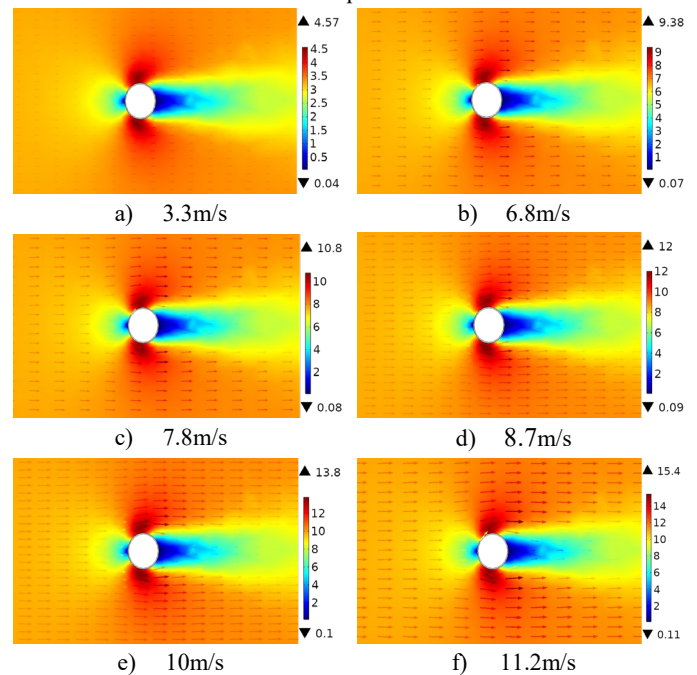c) 7.8m/s              d) 8.7m/s

e) 10m/s               f) 11.2m/s

Fig. 12 The air flow field

It can be seen from Fig. 12 that under the action of different wind speeds, the flow form of the air flow field near the cable-stayed cylindrical structure is basically the same. The greater the wind speed is, the greater the local maximum wind speed of the cable-stayed cylindrical structure is, and the greater the wind speed on the windward and leeward sides of the cable-stayed cylindrical structure is, resulting in the probability of water droplets colliding with the cable-

stayed cylindrical structure becoming greater, so the moisture content of its surface is higher. The moisture evaporation heat absorption is higher, and the critical anti-icing power is increased.

## IV. CONCLUSIONS

The following conclusions were obtained from the critical anti-icing power test at the Xue Feng Mountain Energy Equipment Safety Field Scientific Observation and Research Station and the critical anti-icing numerical simulation analysis of the cable-stayed cylindrical structure:

- The temperature of the leeward side of the cable-stayed cylindrical structure is partially increased compared with the windward side.

- Under the action of the same wind speed, the larger the diameter of the cable-stayed cylindrical structure is, the greater the local maximum wind speed is. The larger the diameter of the cable-stayed cylindrical structure is, the greater the range of the small wind speed on the windward side and the leeward side is, resulting in the probability of water droplets colliding with the cable-stayed cylindrical structure becoming smaller, so the moisture content of its surface is lower. The moisture evaporation heat absorption is lower, and the critical anti-icing power is reduced.

- Under the action of the same wind speed, the local maximum wind speed of the cable-stayed cylindrical structure with different placement angles is basically the same. The larger the placement angle of the cable-stayed cylindrical structure is, the greater the range of the small wind speed on the windward side and the leeward side is, resulting in the probability of water droplets colliding with the cable-stayed cylindrical structure becoming smaller, so the moisture content of its surface is lower. The moisture evaporation heat absorption is lower, and the critical anti-icing power is reduced.

- Under the action of different wind speeds, the flow form of the air flow field near the cable-stayed cylindrical structure is basically the same. The greater the wind speed is, the greater the local maximum wind speed of the cable-stayed cylindrical structure is, and the greater the wind speed on the windward and leeward sides of the cable-stayed cylindrical structure is, resulting in the probability of water droplets colliding with the cable-stayed cylindrical structure becoming greater, so the moisture content of its surface is higher. The moisture evaporation heat absorption is higher, and the critical anti-icing power is increased.

## REFERENCES

[1] X. L. Li, Z. Y. Hao, X. Yang, "Research and accident analysis of national transmission line ice cover," *Urban Construction Theory Research*, iss. 15, pp. 1630-1630, Nov. 2016.

[2] S. Y. Li, T. Huang, J. H. Ye, "Theoretical study on the galloping oscillation stability of ice-covered stay cables," *Vibration and shock*, vol. 32, pp. 122-127, Nov. 2013.

[3] D. M. Tan, S. Z. Luo, W. L. Qu, K. L. Wang, S. M. Mao, "Analysis of three-dimensional fan-shaped ice-covered single-cable and tandem double-cable wind-induced vibration and wake galloping oscillation," *Building Structures*, vol. 49, pp. 120-126, Nov. 2019.

[4] E. F. Teng, Z. D. Duan, X. H. Zhang, "Numerical simulation of aerodynamic characteristics of crescent-shaped ice-covered conductors," *Low Temperature Construction Technology*, iss. 01, pp. 86-88, Nov. 2008.

[5] K. L. Wang, D. M. Tan, W. L. Qu, S. Z. Luo, S. H. Lian, W. H. Zhou, "Two typical ice-covered stayed cable aerodynamic characteristics and galloping oscillation analysis," *Noise and Vibration Control*, vol. 37, pp. 126-131+149, Nov. 2017.

[6] L. E. Kollár, M. Farzaneh, "Wind-tunnel investigation of icing of an inclined cylinder," *International Journal of Heat & Mass Transfer*, vol. 53, pp. 849-861, Nov. 2010.

[7] C. Demartino, F. Ricciardelli, "Aerodynamic stability of ice-accreted bridge cables," *Journal of Fluids and Structures*, vol. 52, Nov. 2015.

[8] T. Huang, "Study on the galloping oscillation stability of ice-covered stayed cable," M. Eng. thesis, Hunan University, Changsha, China, Jun. 2011.

[9] C. L. Bi, "Research on the method of using expanded conductor to prevent ice and snow disasters on transmission lines," M. Eng. thesis, Chongqing University, Chongqing, China, Jun. 2019.

[10] L. C. Shu, J. H. Qi, Q. Hu, "Wind turbine blade electric heating anti-icing model and zonal anti-icing method," *Chinese Journal of Electrical Engineering*, vol. 37, pp. 1448-1455, Nov. 2017.

[11] M. B. Bragg, "Experimental aerodynamic characteristics of an NACA 0012 airfoil with simulated glaze ice," *Journal of Aircraft*, vol. 25, pp. 849-854, Nov. 2015.

[12] G. C. Tang. "Numerical simulation study on hot air anti-icing of inlet branch plate of aero-engine," M. Eng. thesis, Beijing Jiaotong University, Beijing, China, 2021.

[13] J. M. Brown, S. Raghunathan, "Heat Transfer Correlation for Anti-icing Systems," *Journal of Aircraft*, vol. 39, pp. 65-70, Nov. 2002.

[14] G. Zhong, "Numerical simulation of wing-type electrothermal anti-/de-icing system," *Aerospace Manufacturing Technology*, vol. 376, pp. 75-79, Nov. 2011.

[15] K. Z. Ahmed, "Numerical modeling and simulation of hot air jet anti-icing system employing channels for enhanced heat transfer," *King Fahd University of Petroleum and Minerals(Saudi Arabia)*, pp. 1-24, Nov. 2012.

[16] P. B. Mahdi, "Aero-thermal optimization of in-flight electro-thermal ice protectionsystems in transient de-icing mode," *International Journal of Heat and Fluid Flow*, iss. 54, pp. 167-182, Nov. 2015.

[17] B. L. Messinger, "Equilibrium Temperature of an Unheated Icing Surface as a Function of Air-speed," *Journal of Aeronautical Science*, vol. 20, pp. 29-42, Nov. 1953.

[18] T. G. Myers, D. W. Hammond, "Ice and water film growth from incoming supercooled droplets," *International Journal of Heat and Mass Transfer*, vol. 42, pp. 2233-2242, Nov. 1999.

[19] R. J. Roelke, T. G. Jr, K. J. Keith, "De Witt, et al. Efficient Numerical Simulation of a One-Dimensional Electrothermal Deicer Pad," *Journal of Aircraft*, vol. 25, pp. 1097-1105, Nov. 1988.

[20] Q. Hu, X. Y. Yang, B. X. Mei, "Analysis of threshold power density for anti-icing and de-icing of Wind Turbine Blade," *Proceedings of the CSEE2015*, vol. 35, pp. 4997-5002.

[21] C. F. Dong, F. Y. Sun, B. Q. Meng, "A method of fundamental solutions for inverse heat conductionproblems in an anisotropic medium," *Engineering Analysis with Boundary Elements*, vol. 31, pp. 75–82, Nov. 2007.